THREE-DIMENSIONAL GRAVITY MODELING IN ALL SPACE

XIONG LI
BHP Research – Melbourne Laboratories, P.O. Box 264, Clayton South, Victoria 3169, Australia
E-mail: li.xiong.x@bhp.com.au

MICHEL CHOUTEAU
Département de Génie Minéral, École Polytechnique de Montréal C. P. 6079, succ. Centre-ville, Montréal, Québec H3C 3A7, Canada
E-mail: chouteau@geo.polymtli.ca

Abstract. We review available analytical algorithms for the gravity effect and gravity gradients especially the vertical gravity gradient due to a right rectangular prism, a right polygonal prism, and a polyhedron. The emphasis is placed on an investigation of validity, consistency, and especially singularities of different algorithms, which have been traditionally proposed for calculation of the gravity effect on ground (or outside anomalous bodies), when they are applied to all points in space. The rounding error due to the computer floating point precision is estimated. The gravity effect and vertical gradient of gravity in three dimensions caused by a cubic model are calculated by different types of algorithms. The reliability of algorithms for the calculation of gravity of a right polygonal prism and a polyhedron is further verified by using a regular polygonal prism approximating a vertical cylinder and a regular polyhedron approximating a sphere, respectively. By highlighting Haáz-Jung-Plouff and Okabe-Steiner-Zilahi-Sebess' formulae for a right rectangular prism, Plouff's algorithm for a right polygonal prism, and Götze and Lahmeyer's algorithm for a polyhedron and removing their singularities, we demonstrate that these formulae and algorithms can be used to model the gravity anomaly and its vertical gradient at all possible computation positions.

Keywords: three-dimensional body, gravity, gravity gradient, forward modeling, all space, singularity, rounding error

1. Introduction

Gravity meters measure the vertical component of the gravitational attraction, simply and normally called the gravity and denoted by g. For convenience, we adopt two Cartesian systems of coordinates: (ξ, η, ζ) for body coordinates and (x, y, z) for field coordinates. The vertical ζ axis and z axis are taken to be positive downward and the ξ and η axes and the x and y axes are arranged into a right-handed system. The gravity due to a three-dimensional body with density $\rho(\xi, \eta, \zeta)$ and arbitrary shape observed at point (x, y, z) is

$$g(x, y, z) = -G \int\int\int \rho(\xi, \eta, \zeta) \frac{z - \zeta}{r^3} \, d\xi d\eta d\zeta \tag{1}$$

Surveys in Geophysics **19:** 339–368, 1998.

where G is the universal gravitational constant, and

$$r = \sqrt{(x-\xi)^2 + (y-\eta)^2 + (z-\zeta)^2} \tag{2}$$

The simple formula for sphere, cylinder, and other geometrical models can serve very well to give the approximate magnitudes of calculated gravity effects for comparison with the observed values. There are, however, many interpretation problems in which more detailed calculations are useful. Such problems arise, for instance, when it is desired to determine the gravity effect from a geological situation which is partially defined by known stratigraphy and drilling and where the gravity expression is complex but well defined. Three-dimensional methods are preferred, because in general, the anomalies are irregular or do not have a strong elongation in one direction.

There are a number of ways to solve three-dimensional density problems. The popular three categories according to the basic geometrical model used are the stack of right rectangular prisms, the stack of polygonal prisms, and the polyhedron. Traditionally, a method has been developed for surface gravity observations where the computation point is generally outside the body. In the calculation of the gravity effect in a borehole or a tunnel, the formula is especially required to be applicable to all possible computation positions, outside, on the boundary of, and inside the three-dimensional body. An analytical solution is preferred in comparison with the surface gravity, because a numerical quadrature solution, generally, cannot produce a reasonably accurate gravity field inside or near the body.

In Sections 2, 3 and 4 we review the developments of analytical algorithms for the gravity effect due to a right rectangular prism, a right polygonal prism, and a polyhedron, and explain the techniques to remove singularities when the computation point is inside or on the boundary of a prism or a polyhedron. Some cautions in programming are suggested. We have designed a *standard cubic model* combining a three-dimensional observation array so as to check the correctness and consistency of different algorithms. Plouff's (1975, 1976) algorithm for the calculation of gravity of a right polygonal prism is further tested by using an approximation of a 16-side right regular polygonal prism to a vertical cylinder. So is Götze and Lahmeyer's (1988) algorithm for a polyhedron by using a 24-facet regular polyhedron approximating a sphere.

Section 5 is devoted to the description of the rounding error due to the computer floating point precision. We use a cubic model to examine the operational ranges of single and double precision codes.

Section 6 is a general discussion beyond the calculation of the vertical component of the gravitational attraction, including the calculation of the gravity gradient tensor. In Section 7, we present distributions of the vertical gravity gradient in three-dimensional space caused by the standard cubic model and the regular polyhedron.

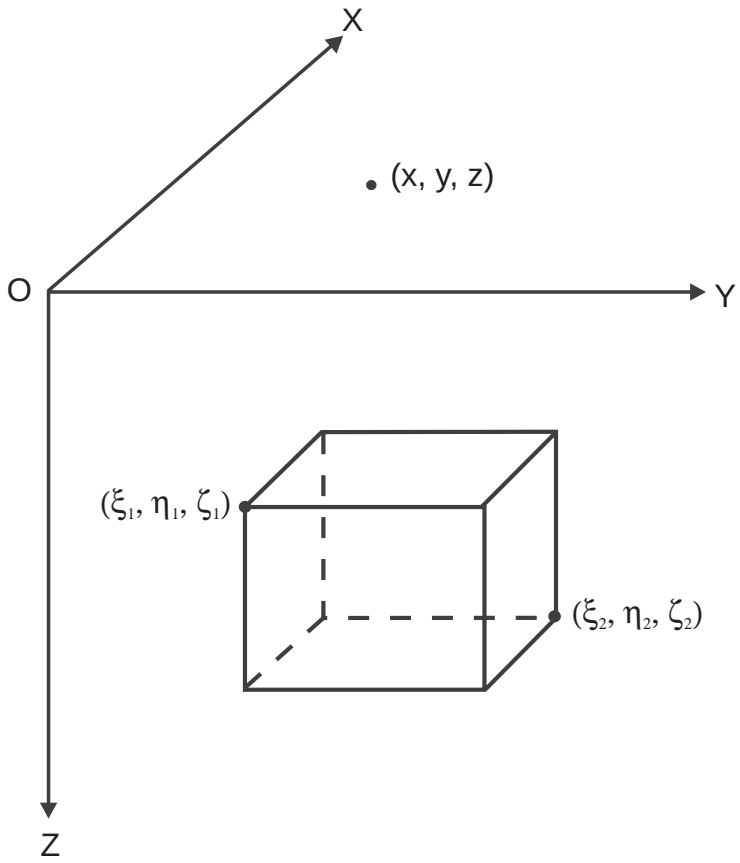

Figure 1. The right rectangular prism model.

2. The Right Rectangular Prism

A collection of rectangular prisms provides a simple way to approximate a volume of mass. If small enough, each prism can be assumed to have constant density. Then by the principle of superposition, the gravitational anomaly of the body at any point could be approximated by summing the effects of all the prisms.

According to Equation (1), a rectangular parallelopiped, which sides of the prism are parallel to x, y, z axes, with uniform density ρ and with dimensions described by the limits $\xi_1 \leq \xi \leq \xi_2$, $\eta_1 \leq \eta \leq \eta_2$, and $\zeta_1 \leq \zeta \leq \zeta_2$ has a vertical attraction at point (x, y, z) (Figure 1) given by

$$g = -G\rho \int_{\zeta_1}^{\zeta_2} \int_{\eta_1}^{\eta_2} \int_{\xi_1}^{\xi_2} \frac{z-\zeta}{r^3} \, d\xi \, d\eta \, d\zeta \tag{3}$$

2.1. DIFFERENT DERIVATIONS

The expression for Equation (3) has been derived by numerous researchers. These analytical formulae have several different forms. The earliest one might be derived by Everest (1830, p. 94–97). He calculated closed-form expressions for the horizontal and vertical gravitational effects of a rectangular parallelopiped and used these equations to estimate the topographic deflection of the plumb bob due to the Satpura Range in India. MacMillan (1930, p. 72–79) gave an analytical formula for computing the potential of this body and discussed the derivation of the three components of gravitational attraction. Another solution was presented by Ansel (1936) both in a closed-form and in the form of an infinite series. He pointed out that for numerical evaluation, a combined use of these two forms is preferred. In fact, his analytical formula represents the gravity effect of a rectangular parallelopiped in the case of $y - \eta_1 = 0$. For the normal cases, to obtain the gravity effect of any rectangular parallelopiped we need to obtain the difference of two rectangular parallelopipeds with a common side in the xz-plane. Kolbenheyer (1963, equation (11)) expressed the vertical component of the attraction of a right prismatical body (a right polygonal prism) as the potential difference between the top and bottom boundary surfaces. Applying his solution to the right rectangular prism, a closed expression for gravity could be derived. Motivated to access errors in computation of gravity terrain corrections, Müller (1963, p. 20) gave an analytical solution which is valid for all possible positions of the right rectangular prism with square top and bottom surfaces.

It is found that Sorokin (1951, p. 370, equation (426)) published an unequivocal solution to this problem. His formula can be written into

$$g = -G\rho \sum_{i=1}^{2}\sum_{j=1}^{2}\sum_{k=1}^{2} \mu_{ijk} \times \left[x_i \ln\left(y_j + r_{ijk}\right) + y_j \ln\left(x_i + r_{ijk}\right) + z_k \arctan \frac{z_k r_{ijk}}{x_i y_j} \right] \tag{4}$$

where

$$x_i = x - \xi_i, \quad y_j = y - \eta_j, \quad z_k = z - \zeta_k \tag{5}$$

$$r_{ijk} = \sqrt{x_i^2 + y_j^2 + z_k^2} \tag{6}$$

and

$$\mu_{ijk} = (-1)^i (-1)^j (-1)^k \tag{7}$$

Several formulae similar to (4) were derived by other researchers. Their difference is only in the last term of (4). Haáz (1953, p. 62) applied Euler's theorem of

homogeneous functions to the second derivative of the potential of a prism, thus obtaining the first derivative and the potential itself without integration. His result for the vertical component of the attraction of a right rectangular prism is

$$g = -G\rho \sum_{i=1}^{2}\sum_{j=1}^{2}\sum_{k=1}^{2} \mu_{ijk} \times \left[x_i \ln\left(y_j + r_{ijk}\right) + y_j \ln\left(x_i + r_{ijk}\right) - z_k \arctan \frac{x_i y_j}{z_k r_{ijk}} \right] \tag{8}$$

Jung (1961) and Plouff (1966, 1975, 1976) derived independently Equation (8) which Plouff used for comparison with terrain correction approximation formulae. The equivalence of Equation (4) and Equation (8) can be easily demonstrated. It is well known $\arctan(a) = \pi/2 - \arctan(1/a)$, the $\pi/2$ terms cancel by the summations.

Nagy (1966) carried out the integration (3) in a different way from Sorokin (1951), in which he used arcsine rather than arctangent expressions, and obtained

$$g = -G\rho \sum_{i=1}^{2}\sum_{j=1}^{2}\sum_{k=1}^{2} \mu_{ijk} \left[x_i \ln\left(y_j + r_{ijk}\right) + y_j \ln\left(x_i + r_{ijk}\right) - z_k \arcsin \frac{y_j^2 + z_k^2 + y_j r_{ijk}}{\left(y_j + r_{ijk}\right)\sqrt{y_j^2 + z_k^2}} \right] \tag{9}$$

Okabe (1979, equation (46)) and Steiner and Zilahi-Sebess (1988) presented another closed-form formula which, like Sorokin's and Haáz, Jung and Plouff's, has an arctangent term. It is

$$g = -G\rho \sum_{i=1}^{2}\sum_{j=1}^{2}\sum_{k=1}^{2} \mu_{ijk} \left[x_i \ln\left(y_j + r_{ijk}\right) + y_j \ln\left(x_i + r_{ijk}\right) + 2z_k \arctan \frac{x_i + y_j + r_{ijk}}{z_k} \right] \tag{10}$$

2.2. Computational aspects

Nagy (1966) wrote, when either the x or y or both axes is crossed (that the x axis is crossed means $\xi_1 \leq x$ coordinate of a computation point $\leq \xi_2$), the integration must be carried out from the lower limit to the axis, then from the axis to the upper limit, the sum of these integration giving the required effect. This means that for an interior point, the prism needs to be divided into four subprisms. This subdivision processing and computational difficulty are due to the use of arcsines

in the expression. It can be avoided by the use of arctangents, e.g., by Sorokin, Haáz-Jung-Plouff, and Okabe-Steiner- Zilahi-Sebess' formulae.

Either Sorokin's formula (Equation (4)) or Haáz-Jung-Plouff's formula (Equation (8)) or Okabe-Steiner-Zilahi-Sebess' formula (Equation (10)) contains 24 terms: 16 logarithms, and 8 arctangents. Their difference is only in the arctangent terms. As a cautionary note, the function ATAN2(a, b) instead of ATAN(a/b) is recommended to use in FORTRAN programming, when one computes the inverse tangent functions in the formulae. Note that the function ATAN2 accepts two arguments which are taken to be, respectively, the ordinate and abscissa of a point in any of the four quadrants. With this additional information, ATAN2 can distinguish the four quadrants and returns an angle in the range from $-\pi$ to π, while ATAN function provides a result in the range of $-\pi/2$ to $\pi/2$ only.

We have designed a cubic model with a unit density (1 g/cm^3) to check the validity and consistency of Haáz-Jung-Plouff and Okabe-Steiner-Zilahi-Sebess' formulae. The lower limits of the cube are $\xi_1 = \eta_1 = \zeta_1 = -10$ m, the upper limits $\xi_2 = \eta_2 = \zeta_2 = 10$ m. The computation points are placed on a three-dimensional grid with a lower bound corner (-20, -20, -20), an upper bound corner (20, 20, 20), and a grid interval (the same in all three directions) 2 m. This arrangement produces an observation array composed of 9261 points. This model is named *the standard cubic model*.

The calculation results show (Figure 2) that the gravity is zero at the $z = 0$ plane, is antisymmetrical about the $z = 0$ plane, is symmetrical about the $x = 0$ and the $y = 0$ planes, and reaches an absolute maximum (346.426 μGal) at the center of the upper or lower boundary surface of the prism. The magnitude of gravity decreases smoothly, when the computation point is away from the body. The FORTRAN single precision codes result in a maximum absolute difference between the two formulae 0.00056 μGal at point (-18, -8, -18) where the calculated gravity is 51.203 μGal. Translating into the relative difference it is about 11 per million. The maximum relative difference is 87.5% which occurs at (18, 10, 0) and at which the calculated gravity fields by two formulae are 0.0001018 μGal and 0.0000127 μGal, respectively. These differences represent the limitation of the floating point precision. Therefore, the value of 87.5% here is meaningless. By the way, all the calculations reported in this paper were done on a SUN Sparc 5.

In conclusion, although Haáz-Jung-Plouff's formula (Equation (8)) and Okabe-Steiner-Zilahi-Sebess' formula (Equation (10)) do not seem to agree, it is verified that they are identical and valid outside, inside, on the boundary of, and even at the vertices of the right rectangular prism.

It is worth to point out that by changing the sign of x_i, y_j, z_k in Equation (5), in other words, by denoting

$$x_i = \xi_i - x, \quad y_j = \eta_j - y, \quad z_k = \zeta_k - z \tag{11}$$

without any other modifications, the gravity calculated by Equations (4), (8), and (10) will not change, will remain the same magnitude and the same sign. This

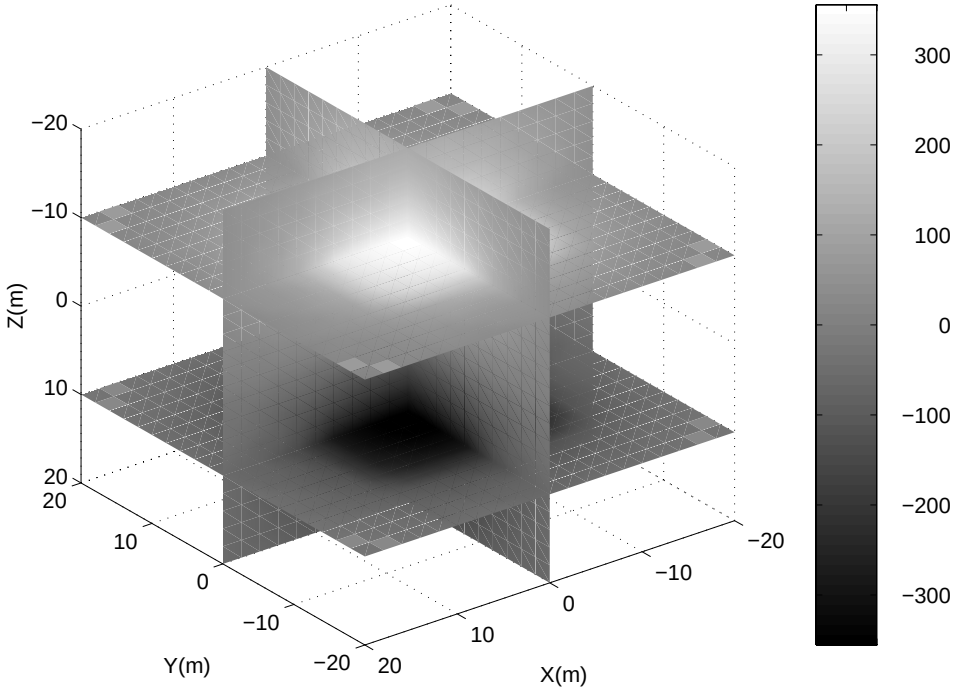

Figure 2. The gravity effect in three dimensions caused by *the standard cubic model* with a unit density (1 g/cm^3), and with the lower limits $\xi_1 = \eta_1 = \zeta_1 = -10$ m and the upper limits $\xi_2 = \eta_2 = \zeta_2 = 10$ m. The gravity is zero at the $z = 0$ plane, is antisymmetrical about the $z = 0$ plane, is symmetrical about the $x = 0$ and $y = 0$ planes, and reaches an absolute maximum (346.426 μGal) at the center of the top or bottom surface of the cube.

fact can be explained from the structure of formulae (Goodacre, 1973). Since the integrand in Equation (3) is an even function of $x-\xi$ and $y-\eta$ and an odd function of $z-\zeta$, the integrated result should be an odd function of $x-\xi$ and $y-\eta$ (but the product of two odd functions is an even function in case of a simultaneous change of their signs) and an even function of $z-\zeta$. At a first glance, neither Equation (4) nor (8) nor (10) seems to satisfy these conditions, but, for example, (8) may be rewritten as

$$g = -G\rho \sum_{i=1}^{2}\sum_{j=1}^{2}\sum_{k=1}^{2} \mu_{ijk}\left[x_i \ln\left(\frac{y_j}{\sqrt{x_i^2+z_k^2}} + \sqrt{1+\frac{y_j^2}{x_i^2+z_k^2}} \right) + y_j \ln\left(\frac{x_i}{\sqrt{y_j^2+z_k^2}} + \sqrt{1+\frac{x_i^2}{y_j^2+z_k^2}} \right) - z_k \arctan\frac{x_i y_j}{z_k r_{ijk}} \right] \tag{12}$$

since

$$\sum_{i=1}^{2}\sum_{j=1}^{2}\sum_{k=1}^{2}\mu_{ijk}\left(x_i \ln\sqrt{x_i^2+z_k^2}\right)=0 \tag{13}$$

and

$$\sum_{i=1}^{2}\sum_{j=1}^{2}\sum_{k=1}^{2}\mu_{ijk}\left(y_j \ln\sqrt{y_j^2+z_k^2}\right)=0 \tag{14}$$

Because

$$\ln\left(\frac{a}{\sqrt{b^2+c^2}}+\sqrt{1+\frac{a^2}{b^2+c^2}}\right)=\arcsin\frac{a}{\sqrt{b^2+c^2}} \tag{15}$$

it is clear that (12) has the desired symmetry property. Equation (9) does not have this property because of the form of the argument in the arcsine term. In practice, we still use (8) rather than (12) because (8) is equivalent to and simpler than (12).

3. The Right Polygonal Prism

Although conceptually straightforward, the right rectangular prism approach would be cumbersome in practice. Geological bodies are often difficult to be modeled with rectangular blocks. Moreover, the computation does not take advantage of the fact that if the densities of neighboring prisms are identical, there is no need to include their mutual interface in the calculation.

Talwani and Ewing (1960) and Talwani (1973) described a more practical method. Their technique approximates a body by a stack of infinitely thin, horizontal laminas. The shape of each lamina is approximated by a polygon. The key formula in this method is to calculate the gravity effect of a horizontal polygon. Grant and West (1965, equations (10–16)) and Golizdra (1981, equation (4)) improved Talwani and Ewing's formula by involving an evaluation of less transcendental functions. Integration over the vertical coordinate is done with numerical quadrature technique. The shorter the height of observation point compared to the thickness represented by each lamina, the more inaccurate the result of the numerical integration will be. The gravity field within or near a lamina cannot be accurately determined by the lamina method (Plouff, 1976).

Plouff (1975, 1976) took this representation one step further. He derived an analytical formula for the gravity effect of a layer of finite thickness, with vertical sides and with top and bottom surfaces approximated by polygons. Analogous to the method of Talwani and Ewing (1960), these polygonal layers can be stacked on

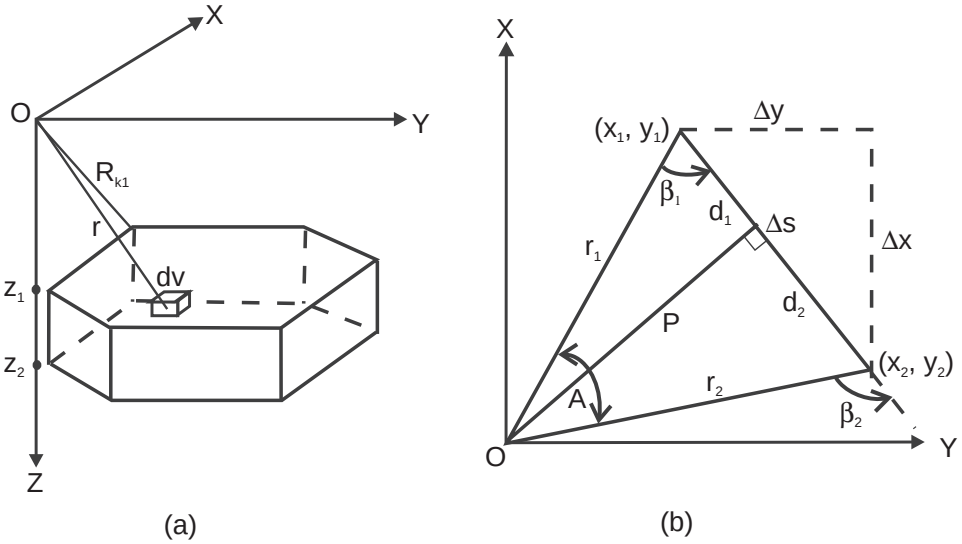

Figure 3. Geometrical elements involved in calculation of gravity anomalies caused by a right polygonal prism. The observation point is located at the origin of the Cartesian coordinate system. (a) a polygonal prism; (b) plan view of one side of prism. (After Plouff, 1976).

top of one another in order to approximate three-dimensional bodies of arbitrary shape.

The geometrical symbols used in Plouff's formula are shown in Figure 3. For the ith edge, the subscript k in R_{kj} refers to the endpoint (or corner) of that edge, and the subscript j the face of the prism. $k = 1$ indicates the first endpoint found in the clockwise progression, $k = 2$ the latter of the two endpoints. $j = 1$ refers to the face closer to the computation point, $j = 2$ the more distant face. The gravity effect of a polygonal prism are expressed in terms of the summation of the contributions from the individual edges of a n-sided prism. The final Plouff's formula for the vertical component of gravity caused by a n-sided right polygonal prism is

$$g = -G\rho s_m \sum_{i=1}^{n} \left[s_p A\,(z_2 - z_1) + z_2 \left(\arctan \frac{z_2 d_1}{P R_{12}} - \arctan \frac{z_2 d_2}{P R_{22}} \right) \right.$$
$$\left. - z_1 \left(\arctan \frac{z_1 d_1}{P R_{11}} - \arctan \frac{z_1 d_2}{P R_{21}} \right) - P \ln \left(\frac{R_{22} + d_2}{R_{12} + d_1} \frac{R_{11} + d_1}{R_{21} + d_2} \right) \right] \tag{16}$$

where P is the perpendicular distance from the computation point to a vertical side of the polygonal prism

$$P = \frac{x_1 y_2 - x_2 y_1}{\Delta s} \tag{17}$$

$$\Delta s = \sqrt{(\Delta x)^2 + (\Delta y)^2} = |d_1 - d_2| \tag{18}$$

and

$$A = \arccos \frac{x_1 x_2 + y_1 y_2}{r_1 r_2} \tag{19}$$

The symbol $s_m = 1$ or -1 depending on if the center of mass of the prism is below or above the computation point. The symbol $s_p = 1$ or -1 depending on if P is positive or negative. For the special case of $P = 0$, the gravity value and area subtended by the corresponding edge of the prism, as viewed from the computation point, are zero. Computer time can be reduced by determining the sum of angles A outside the indicated summation. The sum is 2π for the computation points located over the interior of the polygon, zero for exterior points, π over an edge, and equal to the interior angle if the computation point is located over the intersection of two edges of the polygon.

3.1. TEST USING THE STANDARD CUBIC MODEL

Plouff (1976) already proved that gravity values outside the body obtained by using Equation (16), for any $x - y$ orientation of a right rectangular prism, agree exactly with those obtained by using Equation (8). By using the standard cubic model, our calculation results show that the two FORTRAN single precision codes based on Equation (16) and Equation (8) result in a rms deviation 0.000088 μGal. The maximum absolute difference is 0.000410 μGal at (20, 16, -18) at which the calculated gravity is 31.580 μGal. Or say, the relative difference is 13 per million. The maximum relative difference 50 per million is located at (18, 20, -2) where the gravity has a value of 5.283 μGal. Again, these differences are caused by the floating point precision limitation.

3.2. APPROXIMATION TO A VERTICAL CYLINDER

Furthermore, a vertical cylinder is used to check Plouff's formula. The cylinder has a height of 20 m, a radius of 10 m, and a density of 1 g/cm^3. The gravity response of the cylinder can be analytically estimated. A right regular polygonal prism with 16 sides is inscribed in the cylinder. The prism has the same density as, hence, a smaller mass than the cylinder. Its gravity anomaly calculated according to Plouff's formula is shown in Figure 4. The maximum absolute errors due to the model approximation occur along the vertical axis of the cylinder and are less than 3.1 μGal, about 1% of the maximum gravity anomaly (317.18 μGal) occuring at the center of the top or bottom surface of the prism (Figure 5). Larger relative errors occur, for example, nearly 2% at the vertical location of 20 m and -20 m along the axis. A better gravity approximation can be expected by improving the model approximation, especially by increasing the number of sides of the polygonal prism.

Plouff's formula is valid for any observation positions, outside, inside, on the surface of, and at the corners of the polygonal prism.

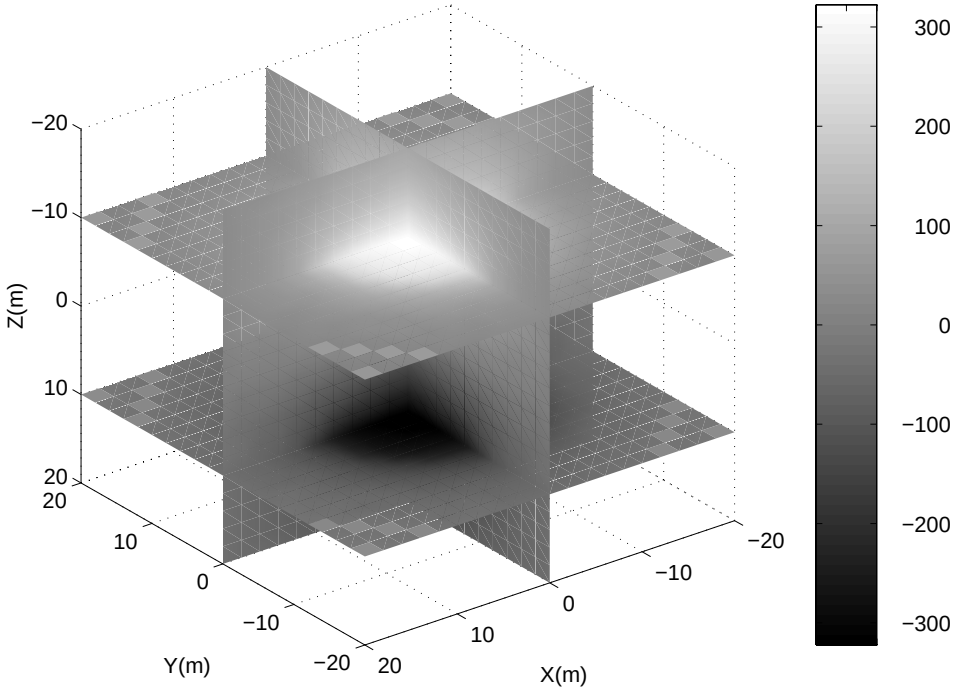

Figure 4. The gravity effect in three dimensions caused by a 16-side right regular polygonal prism approximating a vertical cylinder with a density of 1 g/cm^3, a height of 20 m, and a radius of 10 m. The center of the cylinder or the prism is coincident with the origin of the Cartesian coordinate system.

4. The Polyhedron

It is desirable to compute the gravity effect of any three-dimensional, complex geometrical shape without any need to approximate it by an aggregate of prisms. The analytical evaluation of the gravity effect of a homogeneous polyhedral body has, hence, received wide attention, with notable contributions from Paul (1974), Barnett (1976), Okabe (1979), Götze and Lahmeyer (1988), Pohánka (1988), and Holstein and Ketteridge (1996).

4.1. Development of Algorithms

Bott (1963) might be the first person to suggest such a three dimensional potential-field model: to transform a volume integral into a surface integral, and to approximate representation of the surface by a series of planar polygonal facets. He derived the formulae to evaluate the vertical, horizontal, and total intensity magnetic anomalies due to a uniformly magnetized polyhedron.

Paul (1974) developed a solution of the gravity effect of a homogeneous polyhedron composed of triangular facets. The analytical solution, like the solution for a

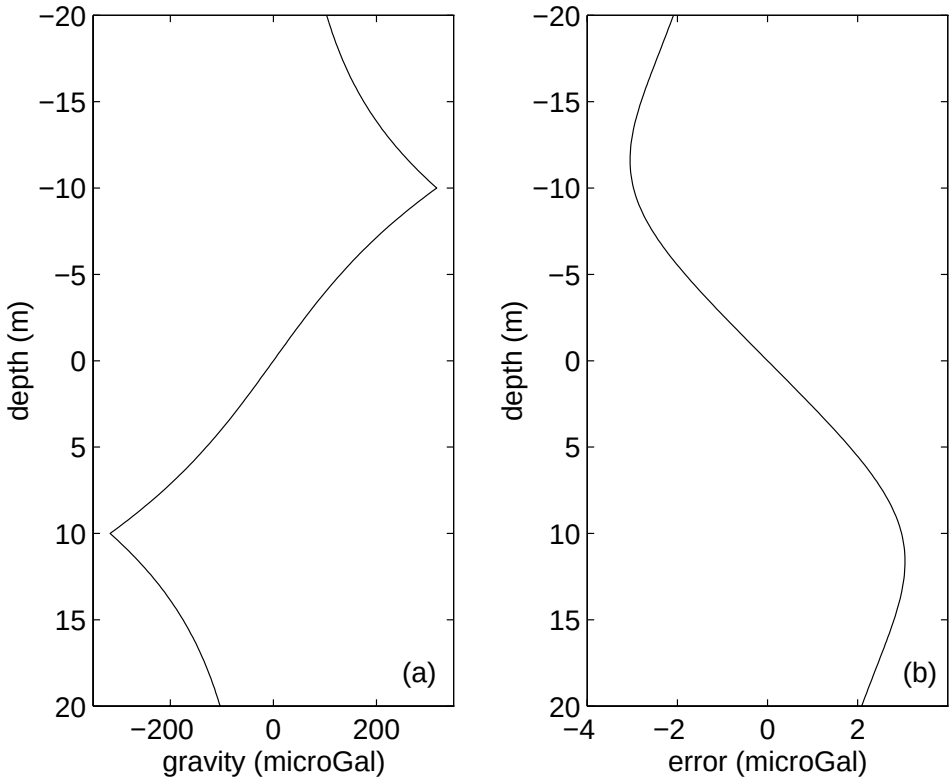

Figure 5. (a) The gravity along the vertical axis of the right regular polygonal prism with 16 sides; and (b) the gravity error due to the approximation of the polygonal prism to the vertical cylinder.

right rectangular prism, is composed of some logarithm and arctangent (or arcsine) functions. Paul used arcsine expressions. The other solutions developed afterwards have widely used arctangents. Paul's solution, like Nagy's (1966) formula, requires a cumbersome procedure to determine the contribution of each facet (i.e., the sign of the various terms) even for external observation points.

Barnett (1976) presented a solution of gravity field based on a very similar polyhedral approach. Especially, he also discretized the surface of the polyhedral body into triangular facets in order to evaluate the required surface integrals. He wrote, "a triangle being the most basic facet shape which can be used to construct facets of any other shape". In programming his key Equation (33), he took precautions to avoid singularities in the logarithm and arctangent expressions. Barnett stated that his formula is equally valid for both external and internal computation points, not valid for points on the surface of the body.

Okabe (1979) criticized the work of Barnett (1976), particularly, the "rather confusing coordinate transformations" used, but Pohánka (1988) pointed out that Okabe's coordinate systems are no better. Ivan (1990) commented on Pohánka's

algorithm, and Pohánka's (1990) reply contains some good viewpoints about numerical precision. Especially, according to Ivan's suggestion, Pohánka (1990) eliminates one logarithm operation.

Okabe (1979) derived analytical expressions of the first and second derivatives of the gravitational potential for a polyhedron composed of planar polygonal facets, not restricted to triangular facets. He used the Gauss' theorem, not like Paul (1974) and Barnett (1976) who applied the direct multiple integral method to the surface integral. Okabe noted the necessity for practical computation to avoid the apppearance of singularities in the logarithm and arctangent terms in his Equation (30) when the observation point is placed on the facet. He removed such singularities in the computer program by using a few appropriate "IF" statements without using the special procedures proposed by Barnett (1976). Therefore, he claimed that his solution is valid everywhere.

Götze and Lahmeyer (1988) independently developed a closed solution for both the gravity field and the vertical gradient of gravity. The difficulty in their approach may be in distinguishing whether a computation point is inside, on or outside the boundary of a triangular facet. Discriminating such cases is time-consuming.

Anyhow, the derivations reported by Paul (1974), Barnett (1976), Okabe (1979), and Götze and Lahmeyer (1988) consist of the common three steps. These are shortly described here. The gravity effect at a computation point caused by a homogeneous polyhedron is the evaluation of the following volume integral

$$g = G\rho \int\int\int_V \frac{\partial}{\partial z}\left(\frac{1}{r}\right) dv \tag{20}$$

where r is the distance between the computation point and the volume element dv. First, transform the volume integral into a surface integral by Gauss' divergence theorem

$$g = G\rho \int\int_S \cos(n, z)\frac{1}{r}\, ds \tag{21}$$

where the cosine term defines the outward normal of the surface element with respective to the z axis. For a polyhedral body, the surface integral is expressed by a sum of contributions from the separate planar polygonal (or triangular) facets S_i ($i = 1, 2, \cdots, m$, the number of facets); and for each facet, $\cos(n_i, z)$ is a constant. Therefore

$$g = G\rho \sum_{i=1}^{m} \left[\cos(n_i, z) \int\int_{S_i} \frac{1}{r}\, ds\right] \tag{22}$$

Next, perform a transformation of coordinate system and define a new Cartesian system in which the z direction is coincident with the direction of outward normal on the surface S_i. Lastly, convert the surface integral in Equation (22) into

a line integral via polygon (or triangle) P_i which limits facet S_i. The final result is obtained inserting the limits of integration (vertex coordinates).

Theoretically, various formulae should lead to the same results. However, in real cases there are many differences: in the number of intermediate computations performed; in the ability of the derived procedures to avoid singularities; and in the efficiency of the computer programming. Mathematically equivalent formulae may give different numerical results. Pohánka (1988) particularly stressed the differences between the exact and numerical evaluation of formulae, and then gave an optimum formula which contains "the smallest possible" number of long operations (logarithms and arctangents). He combined the two arctangents into a single operation, as well as he took care of the values of arguments. His formula (Equation (42)) contains only half as many logarithm and arctangent functions as Okabe's final formula. When the vertical distance z_r between a computation point and a vertex of the polyhedron is zero, it will have zero in the denominator of argument. In order to eliminate the occurance of undefined division in numerical calculation, Pohánka replaced the quantity z_r in the arguments of the logarithm and arctangent functions everywhere by $z_r + \epsilon$, where $\epsilon \geq 0$ has a dimension of length and it is very small relative to the characteristic dimension of the polyhedron. If we choose ϵ appropriately we can reach the numerical result with good accuracy and gain the advantage that we need not care in the division whether the denominator is equal to zero or not. Pohánka's formula is valid not only outside the body but also inside the body and on its surface.

Of the different derivations and formulae, Holstein and Ketteridge's (1996) approach is distinct. When the surface integral over each facet S_i in Equation (22) transforms into a line integral around its boundary, Holstein and Ketteridge differed from previous researchers by replacing the use of the planar Gauss and Green's integral theorems by Stokes' integral theorem. They emphasized a fully vectorial coordinate-free derivation. Hence, their formula has an advantage of algorithmic simplicity over other methods, because of avoiding the need to transform coordinates and the need to discriminate between projected computation points that lie inside, outside, or on a target facet boundary. Moreover, they identified the limitations of a purely analytical formula and suggested a careful choice of numerical and analytical techniques which can particularly overcome the so called rounding error problem.

4.2. THE ASSEMBLY OF POLYHEDRAL BODIES

For practical use, a method must be established to assemble the polyhedron representing the body in a systematical manner. It is quite natural that a polyhedron is first defined by the coordinates of its vertices, and second by the organization of these vertices to form the various facets.

If the facet is defined by a general polygon, not a triangle, it seems that there are no simple and quick ways to assemble a polyhedron. The normal way (Okabe,

1979; Pohánka, 1988; Holstein and Ketteridge, 1996) is to number all vertices, input and store coordinates of the vertices by number, and define each facet by the vertex numbers in anti-clockwise order about the outward facet normal. The latter step is very time-consuming, but particularly necessary in order to obtain contributions of terms with correct sign. Strictly, it is also necessary to determine whether all vertices which represent a polygonal facet are placed on the same plane or not, because the facet can be determined uniquely by only three vertices.

Indeed, if the surface of a homogeneous polyhedral body is discretized into triangular facets, one likely gets poor efficiency because of evaluating more logarithm and arctangent functions compared to the polygonal facet representation. However, it provides a great advantage, i.e., a possibility to automatically generate triangular facets from vertices. Barnett (1976) proposed such a convenient method for assembling a polyhedron. In his method, the polyhedral body is defined by vertices around a series of "slices" through the body. These slices do not have to be either horizontal or planar, but have the single restriction that each slice must contain the same number of vertices. In addition to the slice vertices, a "top" vertex and a "bottom" vertex must be specified. These two vertices, which are included for extra flexibility, may be redundant if the body to be modeled has a flat "top" or a flat "bottom".

In multibody models, how to input polyhedra that would fill all space with no gaps or overlaps becomes more difficult, and the triangular facet integration exhibits its efficiency more. Götze and Lahmeyer (1988) provided a practical technique. The key in their treatment is to divide the whole model into vertical sections (so called planes, they are perpendicular to the main strike direction). The layer boundaries intersected by each plane are determined by a series of points, and each layer boundary consists of triangles which have certain points as their vertices. The program automatically generates the triangular mesh. Götze and Lahmeyer's technique is especially powerful when geological or seismic profile information are available.

4.3. TEST USING THE STANDARD CUBIC MODEL

Götze kindly provided us with a computer program to calculate the gravity effect of a polyhedron composed of triangular facets, which is based on an optimum Götze and Lahmeyer's algorithm (Götze, 1995, unpublished). We used the standard cubic model to check the validity of Götze and Lahmeyer's algorithm.

The calculation results show that the FORTRAN double precision Götze and Lahmeyer's code results in a rms deviation 0.000084 μGal from the FORTRAN single precision code based on Haáz-Jung-Plouff's formula. The maximum absolute difference occurs at (20, 20, 8) and has a value 0.000418 μGal, or 26 per milliom of the calculated gravity -16.653 μGal. The absolute relative difference occurs at (18, 20, -2) and has a value 52 per million of the calculated gravity 5.283 μGal. Once again, these differences are explained by the floating point pre-

cision limitation. Götze and Lahmeyer's algorithm is valid outside, inside, on the boundary of, and even at the corners of the cubic model.

4.4. APPROXIMATION TO A UNIFORM SPHERE

Götze and Lahmeyer's algorithm has been further examined by approximating a uniform sphere with a regular polyhedron. The sphere has a radius of 10 m and a density of 1 g/cm^3. The center of the sphere and the polyhedron is located at the origin of the Cartesian coordinate system. The regular polyhedron consists of 24 triangular facets determined by 14 vertices: (0, 0, 10), (0, 0, −10), (10, 0, 0), (−10, 0, 0), (0, 10, 0), (0, −10, 0), (5.7735, 5.7735, 5.7735) and its 7 mirror symmetrical points. Increasing the number of facets of the polyhedron will decrease the difference between the gravity effect of the sphere and the gravity effect of the polyhedron. The basic characteristics of the gravity field will remain unchanged. It is well known that the vertical component of gravitational attraction outside a sphere is

$$g = -GM\frac{z}{\left(x^2 + y^2 + z^2\right)^{3/2}} \tag{23}$$

where M is the mass of the uniform sphere. The gravity inside the sphere is

$$g = -\frac{4}{3}\pi G\rho z \tag{24}$$

where ρ is the density of the sphere. For the given spherical model, the maximum anomaly in magnitude (279.39 μGal) occurs at the top and bottom points of the sphere.

The regular polyhedron is totally contained by the sphere. The mass of the polyhedron is 2548 tons, 39% less than the mass of the sphere (4189 tons). Hence, it will be expected that the magnitudes of gravity effects produced by the polyhedron are smaller than the ones of the sphere. The gravity approximation can be reduced by improving the model approximation. Figure 6 represents the calculation results for the gravity of the polyhedron using Götze and Lahmeyer's algorithm. Figure 7 demonstrates the difference between the gravity effect of the polyhedron as shown in Figure 6 and the one of the sphere.

Here the computation points are placed on a three-dimensional grid with a lower bound corner (−20, −20, −20), an upper bound corner (20, 20, 20), and a grid interval (the same in all three directions) of 2 m. Under this arrangement, the absolute maximum gravity anomaly (207.61 μGal) is located at point (0, 2, 8) and its 7 mirror symmetrical points. At the top or bottom vertex the gravity has a little smaller value, 200.49 μGal, 28.2% less than the maximum anomaly of the sphere.

The combination of this polyhedral model and three-dimensional computation grid includes almost all possible computation positions relative to all types of

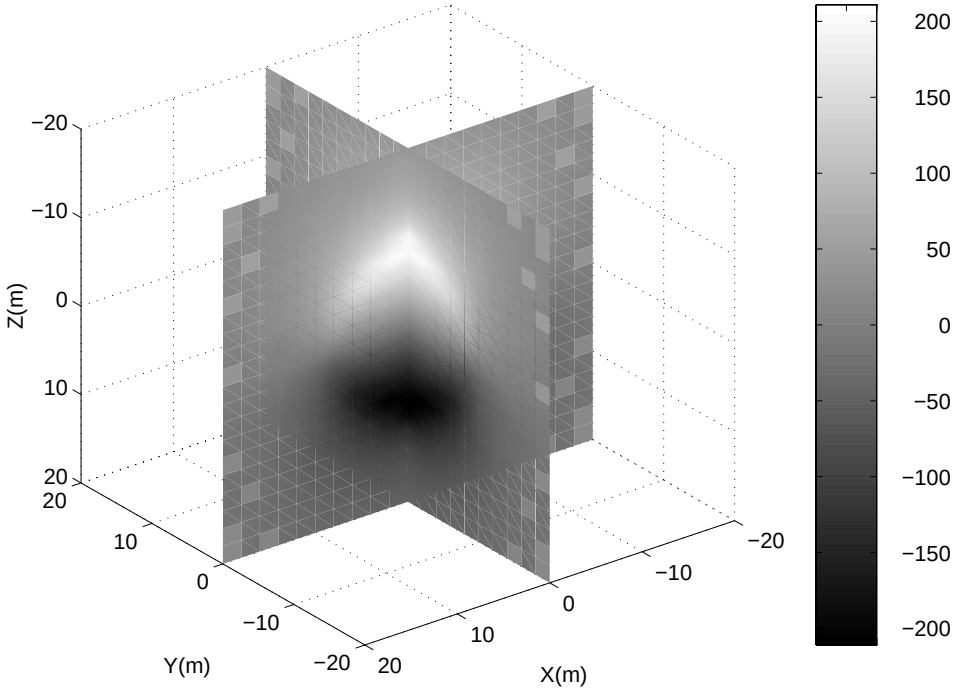

Figure 6. The gravity effect of a regular polyhedron with 24 triangular facets approximating a uniform sphere with a radius of 10 m and a density of 1 g/cm^3, calculated by Götze and Lahmeyer's algorithm. The gravity is zero at the $z = 0$ plane, antisymmetrical about the $z = 0$ plane, symmetrical about the $x = 0$ and $y = 0$ planes, and reaches an absolute maximum near the top and bottom points of the polyhedron.

dipping triangular facets. The calculated gravity effects exhibit the following properties: the gravity is zero at the $z = 0$ plane, antisymmetrical about the $z = 0$ plane, symmetrical about the $x = 0$ and $y = 0$ planes, and has the expected magnitudes. It is reasonably concluded that Götze and Lahmeyer's algorithm results in correct gravity effects at all computation points, outside, at the vertices of, and inside the polyhedron.

5. The Rounding Error

By applying Haáz-Jung-Plouff's formula, Okabe-Steiner-Zilahi-Sebess' formula, Plouff's algorithm and Götze and Lahmeyer's algorithm to the same cubic model, it is demonstrated in the previous three sections that the computer floating point precision influences the numerical calculation of analytical formulae. Generally speaking, analytical formulae for the gravity anomaly of a polyhedral body or a right rectangular prism or a right polygonal prism are subject to numerical error that increases with distance from the target, while the anomaly decreases. This

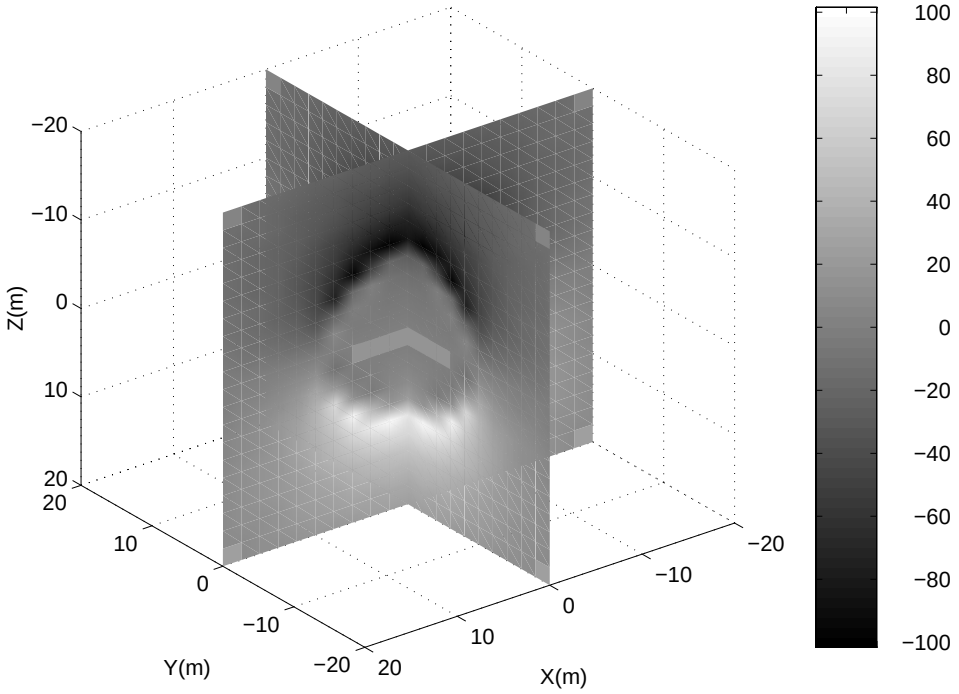

Figure 7. The gravity difference due to the approximation of the regular polyhedron to the sphere. Because the polyhedron is totally contained by the sphere, the gravity effect of the polyhedron has smaller magnitudes.

difficulty leads to a limited range of target distances in which the formulae are operational, beyond which the calculations are dominated by rounding error. This problem was well noticed and solved by Strakhov et al. (1988) and Holstein and Ketteridge (1996).

Following Holstein and Ketteridge's (1996) notations, let α be the typical dimension of the target body, and δ its typical distance from a computation point. Their ratio $\gamma = \alpha/\delta$ defines the (target body) aspect ratio. The calculation of the gravity effect is governed by a volume integral weighted by the inverse square factor $1/\delta^2$, and thus has a magnitude of $O(\alpha^3/\delta^2)$, or equivalently, $O(\alpha\gamma^2)$. Transformation of the volume integral into a sum of surface integrals yields terms of $O(\alpha\gamma)$. Transformation of each surface integral into a sequence of line integrals yields a sum of terms $O(\alpha)$. Transformation of a line integral into analytical primitives (i.e., evaluated at facet vertices, named the analytical vertex method) yields $O(\alpha\gamma^{-1})$.

In summary, the surface integral, line integral and vertex methods generate terms of $O(\alpha\gamma^k)$ for $k = 1, 0$, and -1, respectively. The floating point error of their sum is ϵ (the floating point precision) times this amount, leading to the estimate $O(\alpha\gamma^k\epsilon)$ for the absolute rounding error. Since the vertical component of the

anomaly varies as $O(\alpha\gamma^3)$ in case of substantial foreshortening, the analytical vertex method will avoid error domination only for aspect ratios satisfying $\gamma \gg \epsilon^{1/4}$. The bound on γ depends solely on the floating point precision. It represents a theoretical performance limit of the analytical vertex method, irrespective of the underlying code. Typical values of ϵ for single and double precision are 10^{-7} and 10^{-16}. The bound on γ shows that single precision anomaly calculations with the analytical vertex formula would be error dominated when γ is $10^{-1.7}$ or less, double precision arithmetic even cannot operate at γ below 10^{-4}.

By contrast, Holstein and Ketteridge (1996) extended the performance at a given precision by employing a mix of methods, i.e., the surface method, the line method, and the vertex method, derived from the various integral transformation stages. To combine the best features of the three methods into a single composite algorithm, Holstein and Ketteridge (1996) adopted a decision strategy for switching between surface, line, and vertex methods. The decision tree is:

(1) surface method (numerical quadrature), for $\gamma \gg \epsilon^{1/2}$;
(2) line method (numerical or analytical), for $\gamma \gg \epsilon^{1/3}$; and
(3) vertex method (analytical), for $\gamma \gg \epsilon^{1/4}$.

This decision leads to an efficient, robust algorithm with convergent error.

5.1. NUMERICAL RESULTS

Again, we used the standard cubic model to demonstrate that the analytical methods involve computation of terms that may be arbitrarily large relative to their sum, as $\gamma \to 0$, then limited floating point precision leads to destructive cancellation and ultimate numerical breakdown, and how Holstein and Ketteridge's method can improve performance at large distances. Here the computation points have been arranged as follows: x has values 0, 10, 10^2, 10^3, 10^4, 10^5, 10^6 m, and the same values for y and z. Their combination results in an observation array consisting of 343 points. Haáz-Jung-Plouff's formula (representing the analytical formula for the right rectangular prism), Plouff's algorithm (representing the analytical formula for the right polygonal prism), and Götze and Lahmeyer's algorithm (representing the closed-form formula for the polyhedral body) have been compared. A part of the calculation results is listed in Table I.

The breakdown first occurs for the FORTRAN single precision Haáz-Jung-Plouff and Plouff's codes at computation point (10^3, 10, 10). It occurs for the double precision Haáz-Jung-Plouff's code first at (10^4, 10^2, 10), and for the double precision Götze and Lahmeyer's code first at (10^5, 10, 10). Because the vertical component of the gravitational attraction is calculated, the numerical breakdown occurs at a shorter distance in the horizontal direction than in the vertical direction but where the magnitudes of vertical gravity anomalies have almost the same order. Remember that the linear dimension of the cube tested is 20 m. These numerical results hence indicate that the single precision anomaly calculations with the analytical (vertex) formulae would be error dominated when γ is less than

TABLE I

The numerical breakdown for different codes applied to a cube with an edge of 20 m. x, y, and z are the coordinates of computation points, *Ghps* denotes the FORTRAN single precision Haáz-Jung-Plouff's code for the right rectangular prism, *Ghpd* the double precision Haáz-Jung-Plouff's code, *Gp* the single precision Plouff's code for the right polygonal prism, *Ggl* the double precision Götze and Lahmeyer's code for the polyhedral body with triangular facets, *Ghk* the single precision Holstein and Ketteridge's code for the polyhedron with polygonal facets, and γ is the aspect ratio. The first breakdown for each code is marked in boldface. NaN indicates where the singularity occurs. x, y, and z are in meters, and the gravity in μGal.

x	y	z	*Ghps*	*Ghpd*	*Gp*	*Ggl*	*Ghk*	γ
0	0	0	0.0000763	0.0000233	0.0000000	0.0000000	0.0000000	
0	0	10	−346.4261475	−346.4260254	−346.4260864	−346.4259949	−344.9337158	2
0	0	10^2	−5.3354096	−5.3353801	−5.3351045	−5.3353810	−5.3354244	0.2
0	0	10^3	−0.0533307	−0.0533600	−0.0553662	−0.0533600	−0.0533953	0.02
0	0	10^4	−0.0004071	−0.0005336	0.0000000	−0.0005336	−0.0005337	0.002
0	0	10^5	0.0004071	−0.0000053	0.0000000	−0.0000053	−0.0000053	0.0002
0	0	10^6	0.0000000	−0.0000001	3.3350000	−0.0000001	−0.0000001	0.00002
10	10	10	−129.3164062	−129.3163605	−129.3164062	−129.3163605	NaN	1.1547005
10^2	10	10	−0.5182440	−0.5178795	−0.5179263	−0.5178212	−0.5179033	0.1980295
10^3	10	10	**0.0032568**	−0.0001443	**0.0002620**	−0.0005334	−0.0005351	0.0199980
10^4	10	10	0.0521094	−0.0000003	−0.0079433	−0.0000005	−0.0000005	0.0020000
10^5	10	10	0.0000000	0.0000000	0.0795205	**0.0000008**	0.0000000	0.0002000
10^6	10	10	0.0000000	0.0000000	0.0000000	0.0000279	0.0000000	0.0000200
10	10^2	10	−0.5178369	−0.5178795	−0.5177707	−0.5178212	−0.5178652	0.1980295
10^2	10^2	10	−0.1868610	−0.1872637	−0.1869142	−0.1872460	−0.1873178	0.1410691
10^3	10^2	10	−0.0065137	−0.0010646	−0.0012302	−0.0005256	−0.0005248	0.0198998
10^4	10^2	10	0.0000000	**0.0064784**	−0.1810127	−0.0000005	−0.0000005	0.0019999
10^5	10^2	10	0.0000000	0.0000000	0.0802959	0.0000000	0.0000000	0.0002000
10^6	10^2	10	0.0000000	−0.0000042	0.0000000	−0.0000064	0.0000000	0.0000200

$10^{-1.7}$, and the double precision arithmetic even cannot operate at γ below 10^{-4}. This supports very well Holstein and Ketteridge's (1996) theoretical estimation. Holstein and Ketteridge kindly allowed us to use their single precision composite code. As shown in Table I, their code operates successfully in the whole range assumed. Moreover, we have found that Holstein and Ketteridge's code emphasizes an operating range enhancement, but lacks enough treatments of, for example, singularities. As a result, their code produces a larger computation error at (0, 0, 10) and is singular at a corner of the cube, although an analytical algorithm is adopted for $\gamma \gg \epsilon^{1/4}$.

However, this test allows us to state that the development of algorithms to overcome the rounding error and then to increase the operational range may have only theoretical meaning. In practice and especially in exploration gravimetry, it is always valid to ignore a gravity effect at such a large distance. The maximum gravity anomaly produced by our test cubic model is 346.426 μGal, but the gravity effect is as small as 0.000535 μGal at the first computation point where the numerical breakdown occurs for a single precision code. Equivalently, does anyone care about a gravity effect of less than 1 μGal caused by a tiny or an extremely distant body in the modeling and interpretation of gravity anomalies having a magnitude of 100 mGal? Definitely no.

6. Calculation of Other Gravitational Quantities and Magnetic Field

The Earth's gravitational potential U is a scalar quantity. Its shape can be constrained by its slope in the x, y, and z directions, called the gravitational attraction U_x, U_y, and U_z. In the above sections, we have investigated the analytical calculation of the vertical component of the gravitational attraction U_z or denoted by g. Once a formula is derived to calculate the vertical component of attraction in a Cartesian coordinate system, the x and y components may be obtained by cyclic permutation of the field point and body coordinate parameters. For example, for Haáz-Jung-Plouff's formula (8), we can set $x_i \to y_j$, $y_j \to z_k$, and $z_k \to x_i$, etc. to obtain formulae for the x and y components of the gravitational attraction

$$U_x = -G\rho \sum_{i=1}^{2}\sum_{j=1}^{2}\sum_{k=1}^{2} \mu_{ijk} \times \left[y_j \ln\left(z_k + r_{ijk}\right) + z_k \ln\left(y_j + r_{ijk}\right) - x_i \arctan \frac{y_j z_k}{x_i r_{ijk}} \right] \tag{25}$$

$$U_y = -G\rho \sum_{i=1}^{2}\sum_{j=1}^{2}\sum_{k=1}^{2} \mu_{ijk} \times \left[z_k \ln\left(x_i + r_{ijk}\right) + x_i \ln\left(z_k + r_{ijk}\right) - y_j \arctan \frac{z_k x_i}{y_j r_{ijk}} \right] \tag{26}$$

Gradiometry of potential field anomalies represents a new and encouraging direction which may better constrain the density or susceptibility structure of the earth. As the gravity field is a vector, gravity gradients are represented by a nine component tensor. Because of the symmetrical or irrotational attribute, the gravity gradient tensor is reduced to only six independent components: U_{xx}, U_{yy}, U_{zz} (the vertical gravity gradient), U_{xy}, U_{xz}, and U_{yz}. For the right rectangular prism model, the analytical formulae for the six gravity gradient components, corresponding to Equation (8), are given by (Forsberg, 1984)

$$U_{xx} = G\rho \sum_{i=1}^{2}\sum_{j=1}^{2}\sum_{k=1}^{2} \mu_{ijk} \arctan \frac{y_j z_k}{x_i r_{ijk}} \tag{27}$$

$$U_{yy} = G\rho \sum_{i=1}^{2}\sum_{j=1}^{2}\sum_{k=1}^{2} \mu_{ijk} \arctan \frac{x_i z_k}{y_j r_{ijk}} \tag{28}$$

$$U_{zz} = G\rho \sum_{i=1}^{2}\sum_{j=1}^{2}\sum_{k=1}^{2} \mu_{ijk} \arctan \frac{x_i y_j}{z_k r_{ijk}} \tag{29}$$

$$U_{xy} = -G\rho \sum_{i=1}^{2}\sum_{j=1}^{2}\sum_{k=1}^{2} \mu_{ijk} \ln\left(z_k + r_{ijk}\right) \tag{30}$$

$$U_{xz} = -G\rho \sum_{i=1}^{2}\sum_{j=1}^{2}\sum_{k=1}^{2} \mu_{ijk} \ln\left(y_j + r_{ijk}\right) \tag{31}$$

$$U_{yz} = -G\rho \sum_{i=1}^{2}\sum_{j=1}^{2}\sum_{k=1}^{2} \mu_{ijk} \ln\left(x_i + r_{ijk}\right) \tag{32}$$

To compute higher-order derivatives of the gravitational potential and to analyze singularities of an analytical formula, complex variables theory is proved to be an efficient mathematical tool (Strakhov, 1978; Kwok, 1989). By using the conjugate complex variables formulation, Kwok (1991a, 1991b) derived formulae to calculate the gravity and its x, y, and z derivatives for the right (vertical) polygonal prism, and the first-order derivatives (i.e., the x, y, and z components of the gravitational attraction) and the second-order derivatives (i.e., the gravity gradient tensor) of the gravitational potential due to a homogeneous polyhedron with planar polygonal facets. Kwok's formulae are given in concise formats and include the treatment of the singularities in the integral formulae when the computation point is inside or on the boundary of the body. Therefore, his formulae are valid at all possible points in space.

In principle, any algorithm designed to calculate gravity anomalies can be converted with Poisson's relation into an algorithm to calculate magnetic anomalies. The theory and some applications can be well found in Baranov (1957), Talwani (1965), Goodacre (1973), Okabe (1979), Götze and Lahmeyer (1988), and Blakely (1995).

7. Vertical Gradient of Gravity

In gravimetry, especially in borehole gravimetry, the vertical gradient of gravity is much concerned because the widely-used equation for the determination of (apparent) rock density from borehole gravity data is

$$\rho_a = \frac{1}{4\pi G}\left(F - \frac{\Delta g}{\Delta z}\right) \tag{33}$$

where ρ_a is the calculated density, F is the free-air gradient, Δz is the vertical separation of two adjacent stations, Δg is the difference in gravity readings, and G is the universal gravitational constant. $\Delta g/\Delta z$ can be regarded as a difference approximation of the vertical gradient.

It is well known that the first-order derivatives of (gravitational) potential are continuous everywhere in space, inside, outside, and on the boundary of bodies. The second-order derivatives of potential are continuous everywhere except on the boundary of density variations (see MacMillan (1930, p. 174) for a mathematical explanation). This discontinuity can be well defined by Poisson's equation

$$\frac{\partial^2 U}{\partial x^2} + \frac{\partial^2 U}{\partial y^2} + \frac{\partial^2 U}{\partial z^2} = -4\pi G\rho \tag{34}$$

In other words, the component of the second-order derivatives of potential in the direction normal to a mass interface will have a jump of value of $4\pi G\rho$: it decreases by this amount on entering the body and increases by the same amount on leaving the body.

The vertical gradient of gravity for observation points outside, particularly above infinite or finite masses has been amply discussed. Elkins (1966) gave formulae for the vertical gradient for observations above, inside, and below, but all on the axis of a hollow vertical cylinder and a solid vertical cylinder. LaFehr (1983) treated the so called apparent density anomaly (it is the vertical gradient divided by $-4\pi G$) inside several other simple models, including the nonuniform infinite slab, the circular disc, the uniform sphere, and the uniform infinite horizontal cylinder.

It has been verified by us that Forsberg's (1984) algorithm for a right rectangular prism, Kwok's (1991a) algorithm for a right polygonal prism, and Götze and Lahmeyer's (1988) algorithm for a polyhedron composed of triangular facets produce

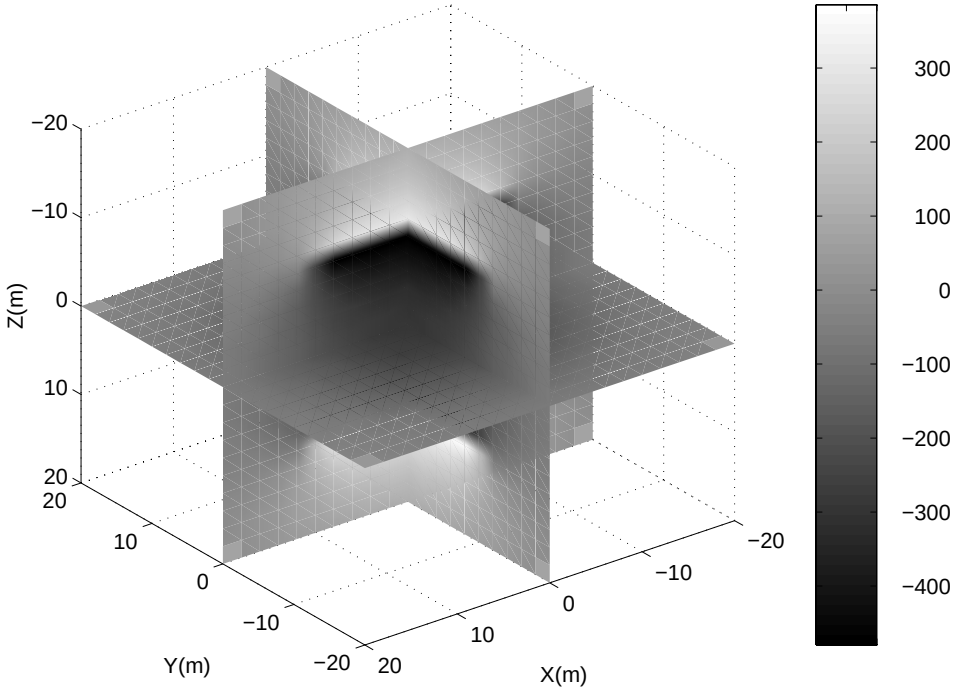

Figure 8. The vertical gradient of gravity due to the cubic model whose gravity effect is shown in Figure 2. It is symmetrical about the $x = 0$, $y = 0$ and $z = 0$ planes. The negative gradient value is constrained within a horizontal layer defined by the top and bottom surfaces of the cube. Elsewhere the gradient is positive. The maximum positive gradient (365.4 Eötvös) and the maximum negative gradient (-472.8 Eötvös) are on the outer side of and the inner side of the top or bottom surface, respectively.

the identical values of vertical gravity gradient outside and inside the right rectangular prism. Figure 8 shows the vertical gradient variation in three dimensions caused by the standard cubic model. Evidently, the variation is continuous everywhere except across the top and bottom boundaries of the cube. This discontinuity or jump is more clearly demonstrated in Figure 9, which represents a profile along the vertical axis of the cube.

We have also calculated the vertical gravity gradient in three dimensions of the previously-adopted regular polyhedral model. The vertical gravity gradient outside a uniform sphere is

$$U_{zz} = -GM\frac{x^2 + y^2 - 2z^2}{\left(x^2 + y^2 + z^2\right)^{5/2}} \tag{35}$$

inside the sphere it is a constant and

$$U_{xx} = U_{yy} = U_{zz} = -\frac{4}{3}\pi G\rho \tag{36}$$

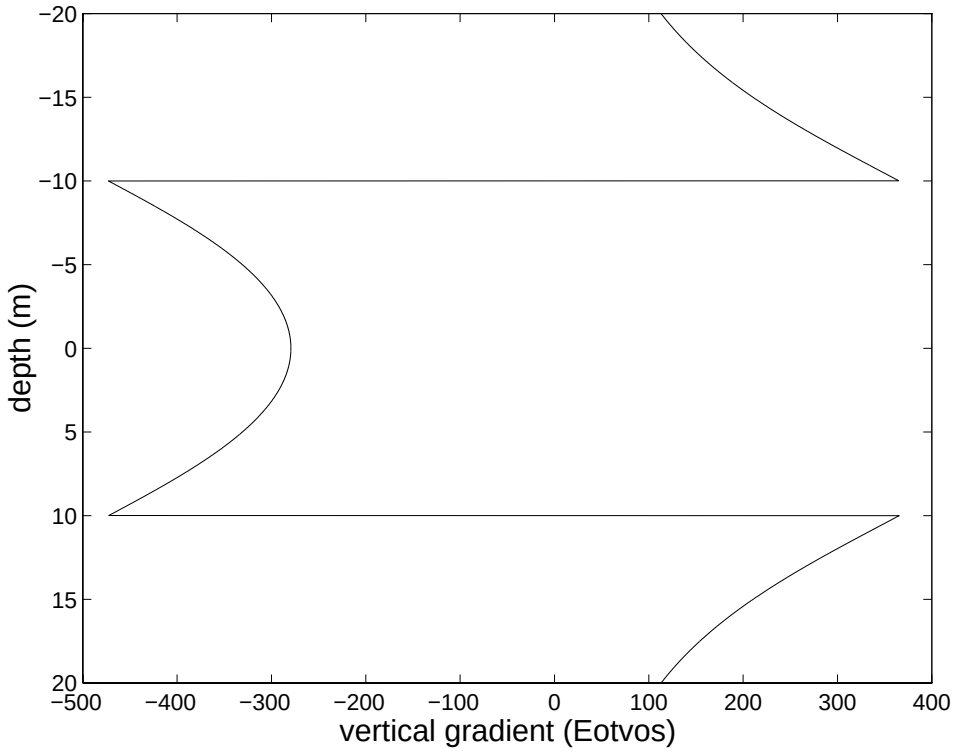

Figure 9. The vertical gradient of gravity along the vertical axis of the standard cubic model.

The maximum jump in the vertical gravity gradient occurs at the top and bottom points of the sphere, and has a value of $4\pi G\rho$ (here, 838.18 Eötvös). Figure 10 represents the vertical gravity gradient of the regular polyhedron calculated by Götze and Lahmeyer's code, and it recovers well the shape and outline of the vertical gravity gradient caused by the test sphere. Due to an interval of 2 m for the computation grid the resolution at the boundary of the sphere or the polyhedron is quite poor. Figure 11 demonstrates clearly the difference between the vertical gravity gradient of the sphere and the vertical gravity gradient of the polyhedron along a profile on the vertical axis of the sphere. The vertical gravity gradient changes largely just outside or inside the body at the top or bottom vertex of the regular polyhedron, but the jump there is less than 400 Eötvös. However, the vertical gravity gradient of the polyhedron reaches the overall minimum around the center of the polyhedron. It has a value -266.24 Eötvös and is close to the minimum vertical gravity gradient of the sphere (-279.40 Eötvös).

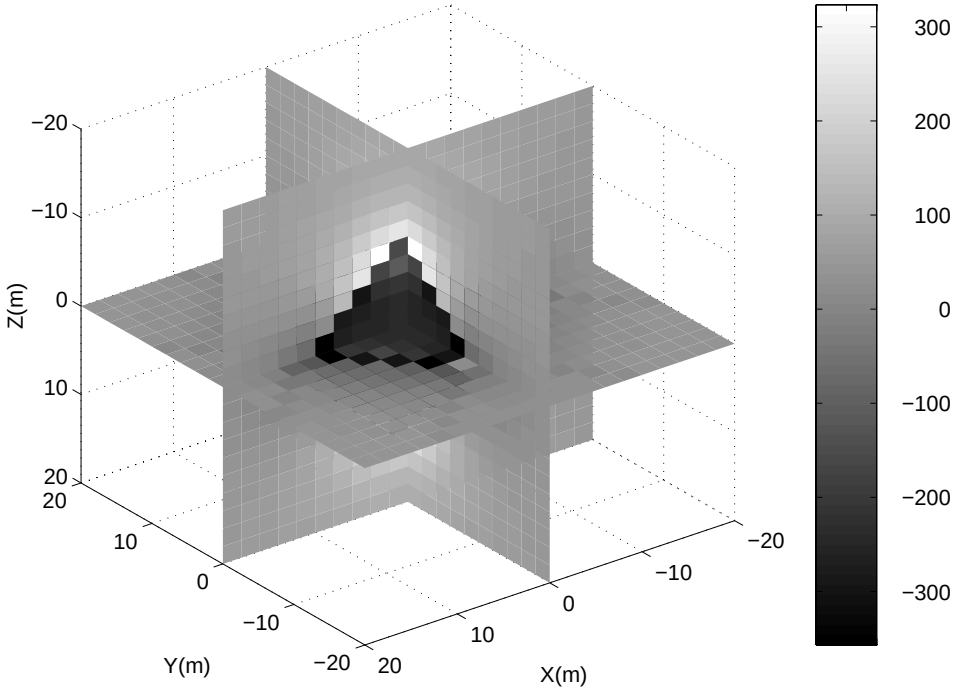

Figure 10. The vertical gradient of gravity due to the regular polyhedron whose gravity effect is shown in Figure 6. Due to the large grid interval of 2 m used in calculation, the gradient is not interpolated and smoothed. The discontinuity at the boundary of the polyhedron is still clear. It keeps well the shape and outline of the vertical gradient of gravity due to a sphere.

8. Conclusions and Remarks

By reviewing available analytical algorithms, we have found that Haáz-Jung-Plouff and Okabe-Steiner-Zilahi-Sebess' formulae, which are different in arctangent terms, for the gravity anomaly of a right rectangular prism yield identical computation results. These three formulae, Plouff's algorithm for a right polygonal prism, and Götze and Lahmeyer's algorithm for a polyhedron with triangular facets have been modified to model gravity effects at all positions, outside, on the boundary of, at the vertex of, and inside the prism or the polyhedron. Singularities are removed by taking precautions in programming, mostly by using appropriate "IF" statements in FORTRAN codes. By applying to representative models, the validity and reliability of these algorithms and formulae have been verified.

Formulae for the calculation of the vertical gravity gradient due to a right rectangular prism (Forsberg, 1984), a right polygonal prism (Kwok, 1991a), and a polyhedron (Götze and Lahmeyer, 1988) have been also verified to be valid and correct both outside and inside the body.

Our test has shown that in practice and even using a single precision code, the rounding error due to the computer floating point precision is insignificant in

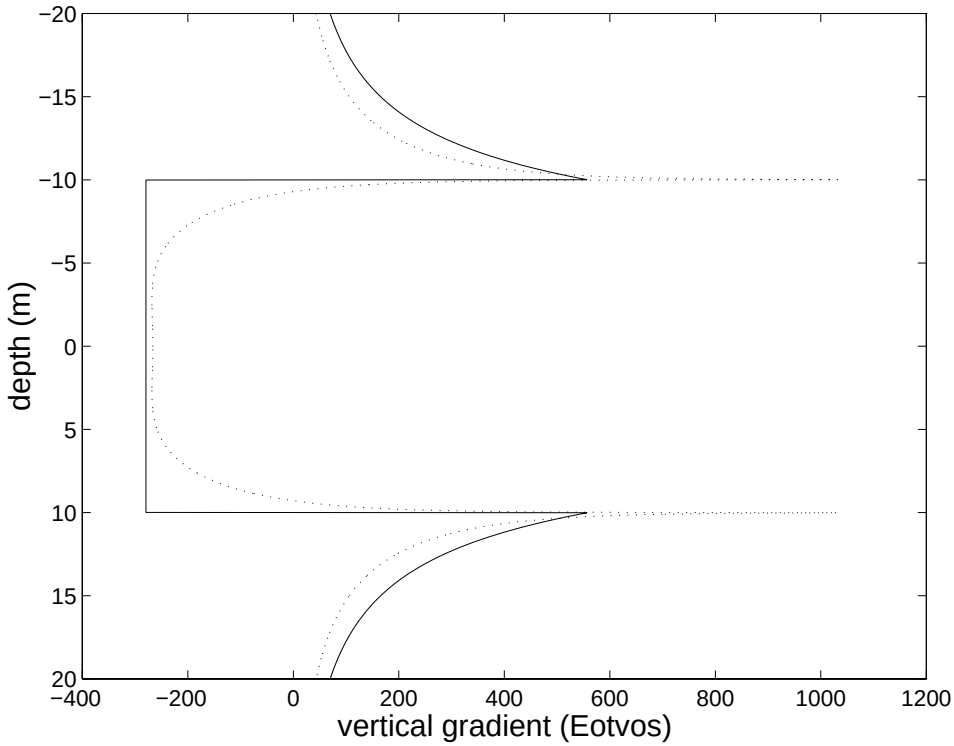

Figure 11. The vertical gradients of gravity due to the sphere (solid line) and due to its regular polyhedron approximation (dashed line) along the vertical axis of the body.

gravity modeling except if the available computer single precision is less than one part in 10^7.

The main principle in choosing the model type in interpretation work is that the more one knows (of the source), the more complex model one uses. Generally, the scale of the problem is not crucial in choosing the model type. The nature has a fractal behaviour and even a hand specimen can show very complex density variations. In order to obtain a quantitative interpretation of three-dimensional subsurface density (contrast) structures, some investigators prefer an automatical inversion of gravity data. In the inversion, the source region is mostly devided into cells (right rectangular prisms).

After gaining more information from field observations, sampling, and drilling, one can, for example, interactively modify the model to be nearly as complex as one will. At that stage one can use a certain modeling algorithm which best suit the complexity of the geological structures. For modeling vertically inhomogeneous bodies, it is difficult to find another method to replace Talwani and Ewing's (1960) approach or Plouff's (1975, 1976) right polygonal prism algorithm. These have led to a variety of computer algorithms specifically designed to model sedimentary structures (e.g., Broome, 1992). The polygonal boundaries could be taken from

stratigraphical contour maps. When modeling complicated bodies, the polyhedral model (Götze and Lahmeyer, 1988; Xia, et al., 1993) may produce a high precision result while requiring relatively less computer time. In order to efficiently assemble polyhedra, triangular facets should be used.

Acknowledgements

We are grateful to H. -J. Götze and S. Schmidt of Freie Universität Berlin and B. Ketteridge of University of Wales Aberystwyth for providing their codes. We also thank P. Keating of Geological Survey of Canada for suggestions. Critical comments and constructive suggestions by an anonymous reviewer are greatly appreciated. This work has been supported by the Natural Sciences and Engineering Research Council of Canada strategic grant STR0181406.

References

Ansel, E. A.: 1936, 'Massenanziehung begrenzter homogener Körper von rechteckigem Querschnitt und des Kreiszylinders', *Beiträge zur Angewandten Geophysik* **5**, 263–295.

Baranov, V.: 1957, 'A new method for interpretation of aeromagnetic maps: pseudo-gravimetric anomalies', *Geophysics* **22**, 359–383.

Barnett, C. T.: 1976, 'Theoretical modeling of the magnetic and gravitational fields of an arbitrarily shaped three-dimensional body', *Geophysics* **41**, 1353–1364.

Blakely, R. J.: 1995, *Potential Theory in Gravity and Magnetic Applications*, Cambridge University Press.

Bott, M. H. P.: 1963, 'Two methods applicable to computers for evaluating magnetic anomalies due to finite three dimensional bodies', *Geophysical Prospecting* **11**, 292–299.

Broome, J.: 1992, 'An IBM-compatible program for interactive three-dimensional gravity modeling', *Computers & Geosciences* **18**, 337–348.

Elkins, T. A.: 1966, 'Vertical gradient of gravity on axis for hollow and solid cylinders', *Geophysics*, **31**, 816–820.

Everest, G.: 1830, *An Account of the Measurement of an Arc of the Meridian Between the Parallels of* $18°3'$ *and* $24°7'$, London.

Forsberg, R.: 1984, 'A study of terrain corrections, density anomalies, and geophysical inversion methods in gravity field modeling', *Report* **355**, *Department of Geodetic Science and Surveying, Ohio State University*.

Golizdra, G. Ya.: 1981, 'Calculation of the gravitational field of a polyhedra', *Izvestiya Academy of Sciences, USSR, Physics of the Solid Earth* **17**, 625–628.

Goodacre, A. K.: 1973, 'Some comments on the calculation of the gravitational and magnetic attraction of a homogeneous rectangular prism', *Geophysical Prospecting* **21**, 66–69.

Götze, H. -J., and Lahmeyer, B.: 1988, 'Application of three-dimensional interactive modeling in gravity and magnetics', *Geophysics* **53**, 1096–1108.

Grant, F. S., and West, G. F.: 1965, *Interpretation Theory in Applied Geophysics*, McGraw-Hill Book Company, Inc., New York.

Haáz, I. B.: 1953, 'Relation between the potential of the attraction of the mass contained in a finite rectangular prism and its first and second derivatives', *Geofizikai Közlemenyek* **2(7)**. (in Hungarian)

Holstein, H., and Ketteridge, B.: 1996, 'Gravimetric analysis of uniform polyhedra', *Geophysics* **61**, 357–364.

Ivan, M.: 1990, 'Comment on "Optimum expression for computation of the gravity field of a homogeneous polyhedral body" by V. Pohánka', *Geophysical Prospecting* **38**, 331–332.

Jung, K.: 1961, *Schwerkraft verfahren in der Angewandten Geophysik*, Akademisches Verlag, Leipzig.

Kolbenheyer, T.: 1963, 'Beitrag zur Theorie der Schwerewirkungen homogener prismatischer Körper', *Studia Geophysica et Geodaetica* no. **3**, 233–239.

Kwok, Y. K.: 1989, 'Conjugate complex variables method for the computation of gravity anomalies', *Geophysics* **54**, 1629–1637.

Kwok, Y. K.: 1991a, 'Singularities in gravity computation for vertical cylinders and prisms', *Geophysical Journal International* **104**, 1–10.

Kwok, Y. K.: 1991b, 'Gravity gradient tensors due to a polyhedron with polygonal facets', *Geophysical Prospecting* **39**, 435–443.

LaFehr, T. R.: 1983, 'Rock density from borehole gravity surveys', *Geophysics* **48**, 341–356.

MacMillan, W. D.: 1930, *The Theory of the Potential*, McGraw-Hill Book Company, Inc., New York.

Müller, P.: 1964, 'Simultane Gravimetrische Bestimmung der Gerteinsdichte und des Schwerefeldes in der Erdkruste, Dissertation ETH, 1963', *Schweizerische Zeitschrift für Vermessung, Kulturtechnik und Photogrammetrie* **62**.

Nagy, D.: 1966, 'The gravitational attraction of a right rectangular prism', *Geophysics* **31**, 362–371.

Okabe, M.: 1979, 'Analytical expressions for gravity anomalies due to homogeneous polyhedral bodies and translations into magnetic anomalies', *Geophysics* **44**, 730–741.

Paul, M. K.: 1974, 'The gravity effect of a homogeneous polyhedron for three-dimensional interpretation', *Pure and Applied Geophysics* **112**, 553–561.

Plouff, D.: 1966, 'Digital terrain corrections based on geographic coordinates', *Geophysics* **31**, 1208.

Plouff, D.: 1975, 'Derivation of formulas and FORTRAN programs to compute gravity anomalies of prisms', *National Technical Information Service* No. **PB-243-526**, U. S. Department of Commerce, Springfield, VA.

Plouff, D.: 1976, 'Gravity and magnetic fields of polygonal prisms and application to magnetic terrain corrections', *Geophysics* **41**, 727–741.

Pohánka, V.: 1988, 'Optimum expression for computation of the gravity field of a homogeneous polyhedral body', *Geophysical Prospecting* **36**, 733–751.

Pohánka, V.: 1990, 'Reply to comment by M. Ivan', *Geophysical Prospecting* **38**, 333–335.

Sorokin, L. V.: 1951, *Gravimetry and Gravimetrical Prospecting*, State Technology Publishing, Moscow. (in Russian)

Steiner, F., and Zilahi-Sebess, L.: 1988, *Interpretation of Filtered Gravity Maps*, Akade'miai Kiado', Budapest, (translated by G. Korvin, Distributed by H. Stillman Publishers, Boca Raton, Florida).

Strakhov, V. N.: 1978, 'Use of the methods of the theory of functions of a complex variable in the solution of three-dimensional direct problems of gravimetry and magnetometry', *Doklady Akademii Nauk SSSR* **243**, 70–73.

Strakhov, V. N., Lapina, M. I., and Yefimov, A. B.: 1986, 'A soultion of forward problems in gravity and magnetism with new analytical expressions for the field elements of standard approximating bodies, I', *Izvestiya Academy of Sciences, USSR, Physics of the Solid Earth* **22**, 471–482.

Talwani, M., and Ewing, M.: 1960, 'Rapid computation of gravitational attraction of three-dimensional bodies of arbitrary shape', *Geophysics* **25**, 203–225.

Talwani, M.: 1965, 'Computation with the help of a digital computer of magnetic anomalies caused by bodies of arbitrary shape', *Geophysics* **30**, 797–817.

Talwani, M.: 1973, 'Computer usage in the computation of gravity anomalies', in B. A. Bolt (ed.), *Methods in Computational Physics* **13**, Academic Press, pp. 343–389.

Xia, H., Hansen, R., Harthill, H., and Traynin, P.: 1993, 'Interactive modeling of potential fields in three-dimensions', *Expanded Abstracts of the 63rd Annual Meeting*, Society of Exploration Geophysicists, pp. 403–404.